General Disclaimer

One or more of the Following Statements may affect this Document

- This document has been reproduced from the best copy furnished by the organizational source. It is being released in the interest of making available as much information as possible.

- This document may contain data, which exceeds the sheet parameters. It was furnished in this condition by the organizational source and is the best copy available.

- This document may contain tone-on-tone or color graphs, charts and/or pictures, which have been reproduced in black and white.

- This document is paginated as submitted by the original source.

- Portions of this document are not fully legible due to the historical nature of some of the material. However, it is the best reproduction available from the original submission.

APOLLO 16 FAR-ULTRAVIOLET IMAGERY AND SPECTRA OF THE LARGE MAGELLANIC CLOUD

Thornton Page

and

George R. Carruthers

COSPAR Paper III. A. 1.8.

Presented at XIXth Meeting of COSPAR

Philadelphia, PA

15 June 1976

E. O. Hulburt Center for Space Research
Naval Research Laboratory
Washington, D. C. 20375

APOLLO 16 FAR-ULTRAVIOLET IMAGERY AND SPECTRA OF THE LARGE MAGELLANIC CLOUD

Abstract

The Large Magellanic Cloud was observed by the Naval Research Laboratory's Far-Ultraviolet Camera/Spectrograph (Experiment S-201) from the lunar surface during the Apollo 16 mission 22 April 1972. Images were obtained with about 3 arc min resolution, in the 1050-1600 and 1250-1600 A wavelength ranges, of nearly the entire LMC. Spectra were also obtained in the 1050-1600 and 900-1600 A ranges along a strip 1/4° wide (determined by the instrument's grid collimator) passing across the LMC. The images and spectra have been scanned with a PDS microdensitometer and isodensity contour plots have been prepared using the Univac 1108 computer at the Johnson Space Center. Comparison with preflight calibrations, verified by observations of the interplanetary and geocoronal Lyman-α emissions, have enabled us to convert the isodensity contour plots to isointensity plots. Model atmosphere predictions of Kurucz, Peytremann, and Avrett, spectral observations of early-type stars in the solar neighborhood with this and other instruments, and the average interstellar extinction curve of Bless and Savage have enabled us to estimate the apparent stellar temperatures and/or interstellar extinction factors which are applicable to the observed early-type star associations in the LMC.

Introduction

The Naval Research Laboratory's Far-Ultraviolet Camera/ Spectrograph (Experiment S-201) was operated on the lunar surface during the Apollo 16 mission 21-23 April 1972. Details of the instrument are given in (1), and some of the other results obtained are given in (2)-(4). One of the targets observed was the Large Magellanic Cloud, in a sequence of exposures beginning 22 April 1972 at 17:18.5 UT and ending at 23:20 the same day. This sequence included direct imagery in the 1050-1600 A and 1250-1600 A wavelength ranges, with exposure times up to 10 min. and 30 min. respectively, and spectrographic exposures in the 900-1600 and 1050-1600 A wavelength ranges, with exposure times up to 30 min. and 200 min. respectively.

The present paper gives a summary of our analyses of these images and spectra to date. A more detailed treatment of the spectrographic observations has been submitted to The Astrophysical Journal, and a more detailed analysis of the direct imagery, including charts and tables of all observed objects in the LMC area, is in preparation.

Data and Analysis

The direct imagery frames from the S-201 instrument covered 20° - diameter circular fields of view and had limiting resolution of about 2 arc minutes at field center, degrading to about 4 arc minutes near the edges. The LMC was near the edge of the field in those frames in which it appeared, hence the resolution was typically

3 to 4 arc min. Exposures were taken with a LiF corrector on the electrographic Schmidt camera (ILi exposures, wavelength range 1050-1600 A) and with a CaF_2 corrector (ICa exposures, wavelength range 1250-1600 A). Fig. 1 is a comparison of the 10- min. ICa exposure (Frame A129) with a ground-based visible-light photograph.

In the spectrographic mode, the field of view was determined by an electroformed-grid collimator placed ahead of the objective grating, giving a triangular response of $1/4^{\circ}$ full width at half maximum in the dispersion direction, with the full 20° field of view along the dispersion (however, the effective transmission of the collimator decreased toward the limits of the 20° field). The field of view along the dispersion corresponded to a spectral resolution of about 30 A in exposures using the LiF corrector plate (SLi exposures, wavelength range 1050-1600 A) but was degraded to about 40 A in exposures without the corrector (SO exposures, wavelength range 900-1600 A).

The data frames were analyzed by scanning the flight films with a Boller and Chivens PDS microdensitometer. A raster scan of 1024 by 1024 elements at 33 micron (1.19 arc min.) intervals was used, and the quantity recorded on magnetic tape was optical density $d=\log_{10} I_o/I$. An asset of the electrographic recording technique is that the optical density of the processed emulsion is directly

proportional to integrated photon flux up to densities of about 1.5, and the density-exposure relationship can be usefully determined to densities above 3.0. Preflight laboratory calibrations of the instrument's spectral response and absolute sensitivity were used to determine the ultraviolet brightnesses of observed diffuse and point sources. Observations of the hydrogen geocoronal and interplanetary Lyman-α emissions (3) are consistent with other measurements of these emissions, and hence tend to confirm the preflight calibrations.

The PDS tapes were analyzed on the Univac 1108 computer at the Johnson Space Center, to produce isodensity contour plots (see Figs. 2 and 3). The densities were typically smoothed, by a weighted averaging process between the particular picture element and the surrounding 12 pixels. Also, the density could be "linearized" by correcting for the nonlinearity of the density-exposure relation and for the lag in the microdensitometer response at high densities.

For a point source image, the integrated intensity could be determined by obtaining the density volume, $V = \Sigma(D_L - B_L)$, where D_L is the linearized density (x 100) of a pixel in the image under consideration, and B_L is the linearized background density (x 100) near, but outside of, the image. In the LMC, determination of the true background density is particularly difficult because of the multitude of field stars against which a particular association or other object in the LMC must be observed. We obtained density volumes for all of

the point-like images in the LMC which could be identified with OB associations of Lucke and Hodge (6) or emission nebulae catalogued by Henize (7), as well as for 140 other areas bright in our far-UV imagery, and for 18 catalogued foreground stars of spectral types B9 to A3 (see Table 1).

Using Henize's estimates of Hα surface brightnesses calibrated by Doherty et al. (8), we calculated the Hα flux from each emission region and its ratio to the measured far-UV flux (see Fig. 4). This "hydrogen index" is zero or very near zero for the 35 associations and 140 other hot-star areas far from Hα emission regions. The small, faint Henize nebulae have hydrogen index about 0.05 to 0.1, which indicates the upper limit of Hα emission not detected by Henize. Values of 6.8 to 21.0 are reached in several areas near 30 Dor. Some of them are small nebulae in which interstellar dust extinction cuts down the far-UV flux, but others (N163 with index 19.7) are fairly large (6 x 6 arc min). Measurements of some of these areas have also been made longward of 1500 A with the ultraviolet spectrometer on board the ANS spacecraft (9).

To compare the observed far-UV fluxes with expectations, the camera response in the direct imaging mode was folded with model atmosphere calculations of Kurucz et al. (10) and the "average" far-UV extinction curve of Bless and Savage (11). It must be cautioned that these predictions may not be totally applicable to the Large Magellanic Cloud, because there are indications that the interstellar extinction curve in the LMC may be anomalous (9),

and if there is a deficiency of heavy elements vs. hydrogen in the LMC, there may be less line blanketing in the stellar far-UV spectra than for galactic early-type stars, and hence the model atmosphere predictions may not be accurate.

Fig. 5 is the computed star magnitude required to produce a density volume of 5131, for the various exposures, vs. unreddened model effective temperature. This "standard" density volume corresponds to a conical image with peak density of 1.0 and 7 rasters full width, and is by no means the weakest measureable image (density volumes less by at least a factor of 100 are accurately determinable). Unfortunately, it is not practical to separate the effects of temperature and of interstellar extinction using the UV imagery data alone, as the effect of extinction is very nearly equivalent to a decrease in effective temperature in the wavelength range covered by the ILi and ICa exposures. Only if the reddening and/or effective temperature is known from ground-based measurements can the UV fluxes be used to provide independent estimates of temperature and far-UV extinction. Although Lucke (12) has estimated the extinction for some of his associations, and Bok and Bok (13) have measured integrated visual magnitudes and B-V colors for some associations, comparison of the present UV data and ground-based data is difficult because of the incompleteness of the available ground-based data and the fact that the S-201 measurements integrate over areas which are larger than the individual associations, and hence include a large contribution due to field stars.

Fig. 6 shows the location of the spectrograph "slit" projected on the direct imagery isodensity contour plot from Frame A129. The location of the slit is uncertain by up to $1/8^{\circ}$, and the region of the LMC contributing to the observed spectra is roughly $1/4^{\circ}$ (along the dispersion) by $1/8^{\circ}$ (transverse to the dispersion). Hence, isolation of the contributions of individual associations is even more difficult than in the direct imagery. However, it appears that the main contribution to the spectrum at the No. 1 maximum is due to the associations NGC 2050 and 2055 (LH 93, 94, 96).

As in the direct imagery, model atmosphere flux distributions and the interstellar extinction curve were folded with the instrumental response in spectrographic mode. The resulting calibration was confirmed by the close agreement of an S-201 spectrum of the AOV star θ Cap with a 9500K unreddened model. The spectral distribution of LMC No. 1 seems consistent with a Kurucz et al. model with T_e=30,000 K, combined with an extinction corresponding to E(B-V)= 0.3, but a variety of combinations with different temperatures and extinctions are possible. The above combination predicts a combined visual magnitude of 7.25, which is somewhat brighter (by about 0.6 mag) than expected based on integrated brightnesses of associations by Bok and Bok.

The integrated density volume of NGC 2050 (LH 93) and NGC 2055 (LH 94) on direct-imagery frame A129 (see Table 1) is 17,050. Using Fig. 5, and assuming linearity, we find

that this corresponds to 7.3 visual magnitude if due to 13,000 K unreddened stars, or 30,000 K stars with E(B-V)= 0.3, in good agreement with the results of the spectra.

Conclusions

The S-201 experiment has returned far-UV imagery data covering most of the Large Magellanic Cloud with 3 to 4 arc min resolution. These data have yielded far-UV brightnesses of catalogued OB associations and Hα emission regions, as well as many other stars or star groupings in the LMC (plus foreground stars in our own Galaxy). At present, the task of comparing, in detail, the far-UV measurements with ground-based measurements has just begun, and a complete catalog with charts and tables is in preparation.

The S-201 instrument also obtained spectra in the 900-1600 and 1050-1600 A ranges of a strip about 1/4° wide crossing the LMC, with 40 A or 30 A spectral resolution and with a spatial resolution of about 1/8° transverse to the dispersion. Both the spectra and the direct imagery of the region of NGC 2050-2055 are consistent with an effective temperature of 30,000 K, reddened by E(B-V)= 0.3, and an integrated visual magnitude of about 7.3.

We thank Richard Hill or Lockheed Electronics Corp. in Houston for his assistance in the computer analysis of the data and the preparation of the isodensity contour plots. We thank Dr. Karl Henize for useful discussions. The S -201 data analysis is supported by NASA contract DPR-H-1304-3B.

REFERENCES

(1) G. R. CARRUTHERS, Appl. Opt. 12, 2501 (1973).

(2) G. R. CARRUTHERS and T. PAGE, J. Geophys. Res. 81, 483 (1976).

(3) G. R. CARRUTHERS, T. PAGE, and R. R. MEIER, J. Geophys. Res. 81, 1664 (1976).

(4) G. R. CARRUTHERS and T. PAGE, J. Geophys. Res. 81, 1683 (1976).

(5) G. R. CARRUTHERS and T. PAGE, Astrophys. J. 205, 397 (1976).

(6) P. B. LUCKE and P. W. HODGE, Astron. J. 75, 171 (1970).

(7) K. G. HENIZE, Astrophys. J. Suppl. 2, 315 (1956).

(8) L. DOHERTY, K. G. HENIZE, and L. H. ALLER, Astrophys. J. Suppl. 2, 345 (1956).

(9) J. BORGMAN, R. J. VAN DUINEN, and J. KOORNNEEF, Astron & Astrophys. 40, 461 (1975).

(10) R. L. KURUCZ, E. PEYTREMANN, and E. A. AVRETT, Blanketed Model Atmospheres for Early Type Stars, Smithsonian Press, Washington, 1974.

(11) R. C. BLESS and B. D. SAVAGE, Astrophys. J. 171, 293 (1972).

(12) P. B. LUCKE, Astrophys. J. Suppl. 28, 73 (1974).

(13) B. J. BOK and P. F. BOK, M.N.R.A.S. 124, 435 (1962).

TABLE I. SOME OBSERVED HOT STAR GROUPINGS

IN THE LARGE MAGELLANIC CLOUD

(S-201 ICa 10 MIN. EXPOSURE, FRAME A 129)*

Henize Nebula	Lucke Hodge Ass'n	NGC	1950 α	1950 δ	Neb Size NSxEW (arc-min)	Hα Flux	Ass'n Size NSxEW (arc-min)	No. of Blue Stars	10mICa Corrected D-Volume
N48 A,B,C	52,53	1948	$5^h25.7^m$	$-66^\circ19'$	1.3x0.9	4.27	4.5x4.5 19x6	15 19	32
N55, A	72		32.7	-66:28	7.2x4.6	173.3	6x3	16	1273
--	77	2002,06,27,34	33.3	-66:59		0	5x30	138	~15000
N51A,C	60	Bok 1968	27.8	-67:30	1.5x1.4	15.5	3x6	16	245
N57A,E	76	Bok 2014	32.1	-67:44	0.9x0.7	126.2	3.5x6	34	3663
N59,A,B,C	88 82	2040 2029,32,35	35.0	-67:35	9.3x7.5	447.2	2x2 6x3	9 ?	873
N157A,B	100	2070	39.0	-69:06	17.7x15.4	3719.	9x9	?	9934
--	96	2050,55	37.4	-69:25		0	10x17	226	~17050
N154B	81	2033	34.9	-69:48	0.1x0.1	~1.	5.5x4.5	49	~60
N160,A-D	103	2077,80, 85,86	40.8	-69:38	15x14	771.9	4x5	41	1007
N159A-L	105	2078,79,83,84	40.4	-69:46	7.2x7.2	102.6	4x4	?	(-54)
N158A	104	2081	40.6	-69:24	0.9x0.8	5.9	6x3.5	48	158

*These also fall in or near the spectrographic mode field of view (Fig. 6).

FIGURE CAPTIONS

FIGURE 1. Comparison of a far-ultraviolet (1250-1600 A) image of the Large Magellanic Cloud (Frame A129) with a ground-based visible-light photograph (courtesy of Lick Observatory). Note that the central "bar" of the LMC, which consists mainly of late-type stars but is the brightest part in visible light, is inconspicuous in the far UV relative to the outer regions, which are rich in early-type stars.

FIGURE 2. Isodensity contour plot of the region of Frame A129 containing the Large Magellanic Cloud. The contour interval is .10 density. The axes of the plot are x and y rasters (256 in each direction), and the angular scale is $.02^{\circ}$/raster. North is to the right.

FIGURE 3. Isodensity contour plot from S-201 spectrographic Frame 140 (200-min. SLi) in the LMC. This plot covers x and y intervals of 256 rasters, and contour interval is .05 density. Wavelength increases from the bottom; dispersion direction is rotated about 11° relative to the y (cross-film) direction. Wavelength range is 1050-1600 A. Note intense interplanetary Lyman-α (1216 A) emission which extends across the field of view. Numbered maxima are identified in Fig. 6. "S" and "G" denote image artifacts.

FIGURE 4. Hydrogen index (dimensionless ratio of Hα to UV flux) for selected areas of the LMC, computed from measurements on Frame A129.

FIGURE 5. Stellar visual magnitude vs. effective temperature to produce a "standard" density volume of 5131, for various S-201 exposures, computed from models of Kurucz et al. and the preflight S-201 instrument calibration, assuming no interstellar extinction.

FIGURE 6. Orientation of spectrograph slit relative to an isodensity contour plot from S-201 direct imagery of the LMC in the 1250-1600 A wavelength range. An approximate RA-DEC grid is superimposed. The dashed line indicates the upper limit of the spectrographic field of view with nominal displacement of 1/8° above the nominal position.

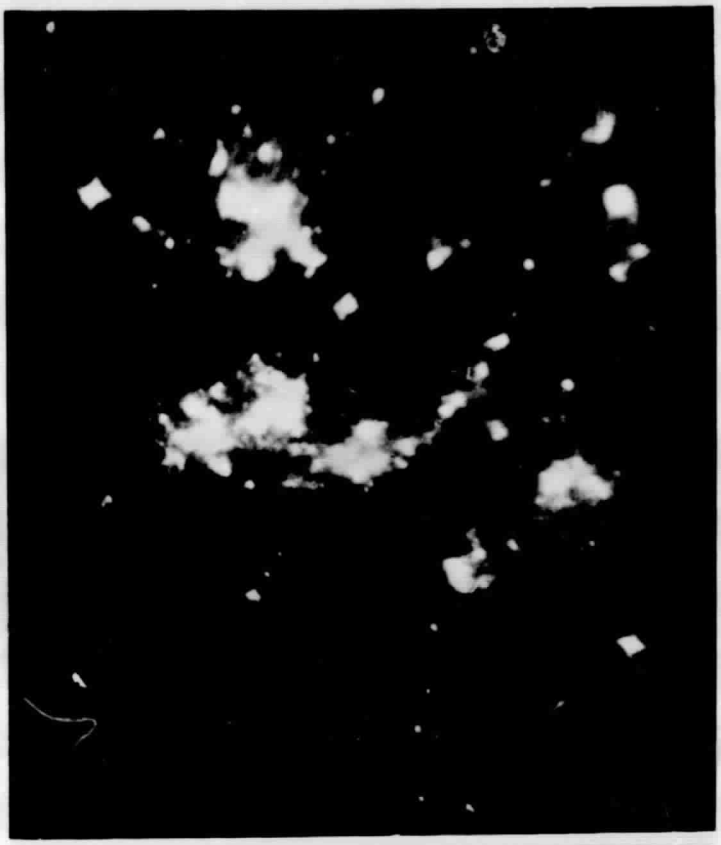

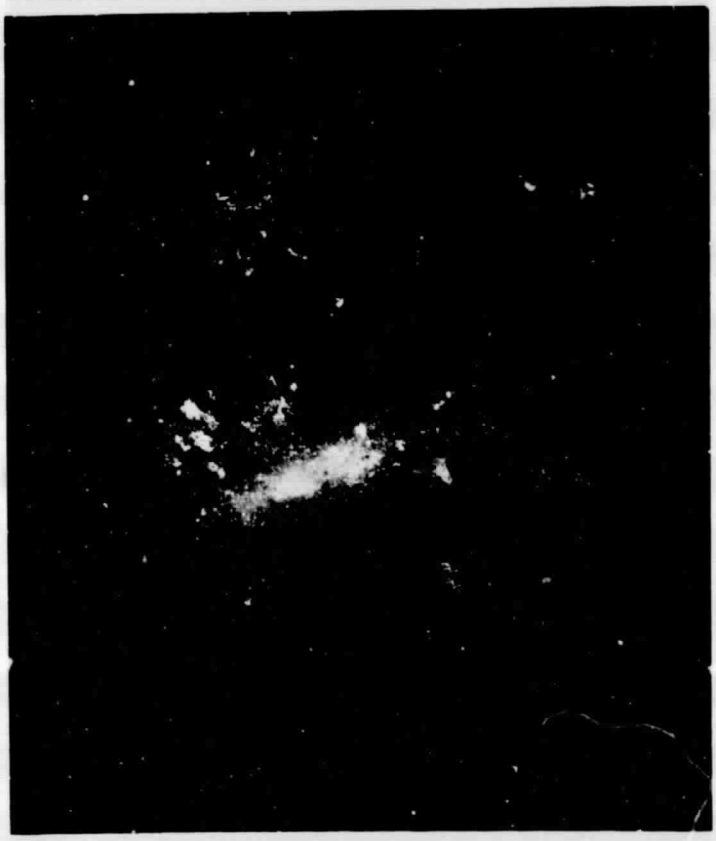

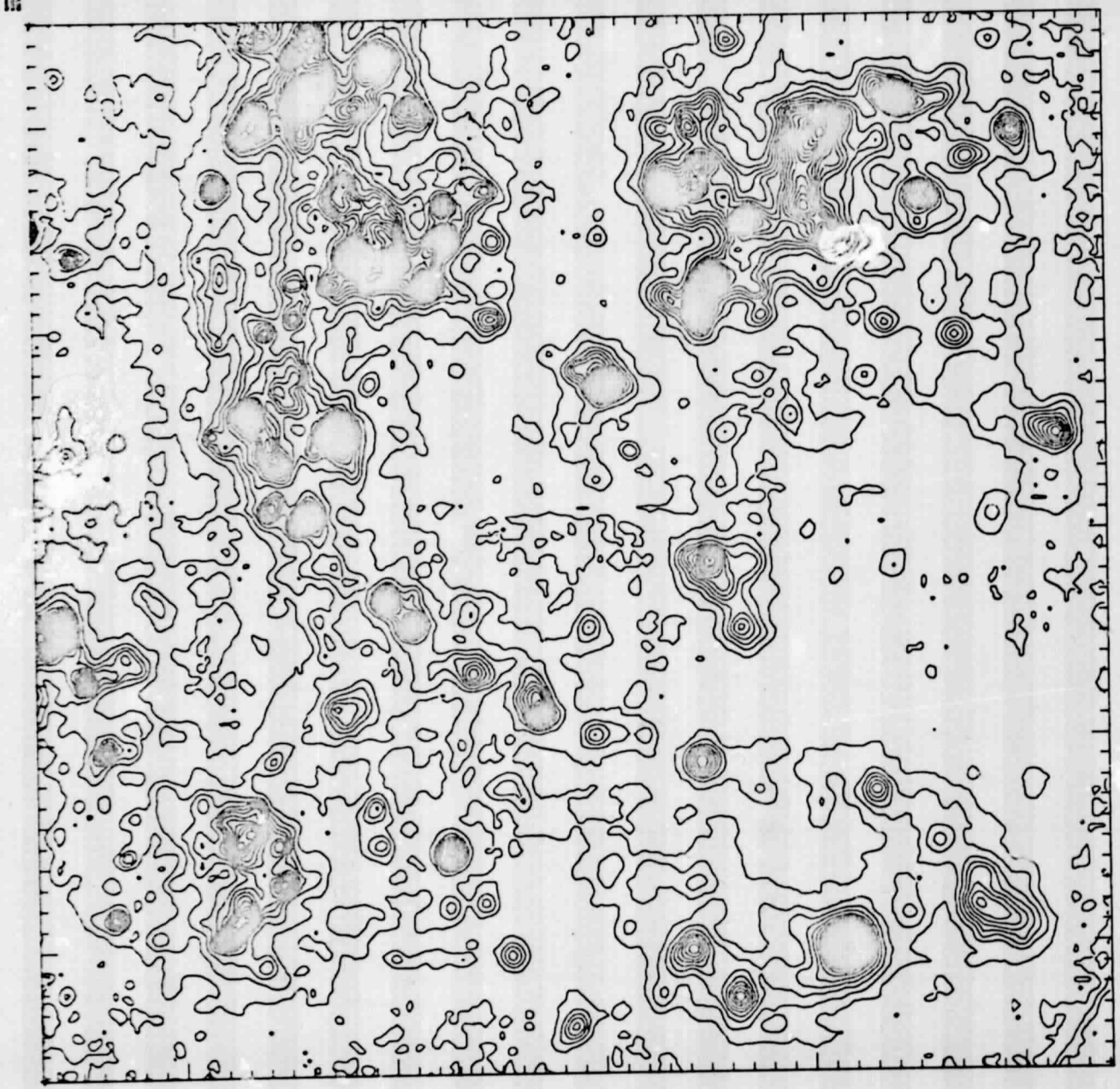

S201
UV CAMERA EXPERIMENT
MISSION FRAME 129
TARGET: L MAG. CLOUD
EXPOSURE TIME: 10.00
EXPOSURE DATE: 04/22/72

SCAN SPEED 30
DENSITY X 100
SMOOTHED DATA

MIN/MAX X COORD. 665 , 920
MIN/MAX Y COORD. 525 , 780
X/Y INTERVAL 33 , 33
MINIMUM CONTOUR LEVEL 20
MAXIMUM CONTOUR LEVEL 400
CONTOUR INTERVAL 10

S201
760051

04/27/75
V16986

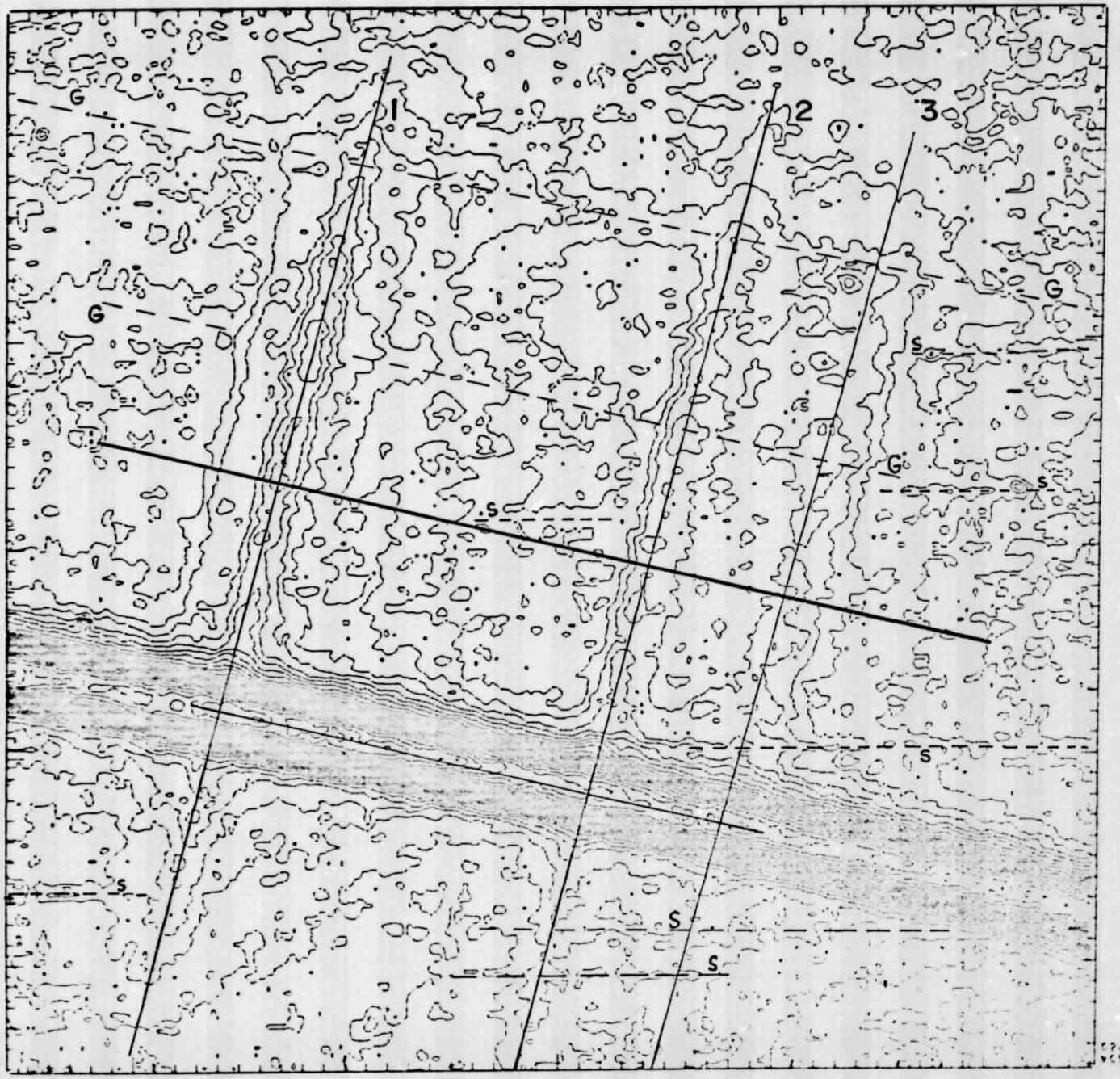

S201
UV CAMERA EXPERIMENT
MISSION FRAME 140
TARGET L MAG. CLOUD
EXPOSURE TIME 200.00
EXPOSURE DATE 04/22/72

SCAN SPEED 30
DENSITY X 100
SMOOTHED DATA

MIN/MAX X COORD. 670 , 925
MIN/MAX Y COORD. 420 , 675
X/Y INTERVAL 33 , 33
MINIMUM CONTOUR LEVEL 6
MAXIMUM CONTOUR LEVEL 151
CONTOUR INTERVAL 5

SEN CORRECTED

S201
760044

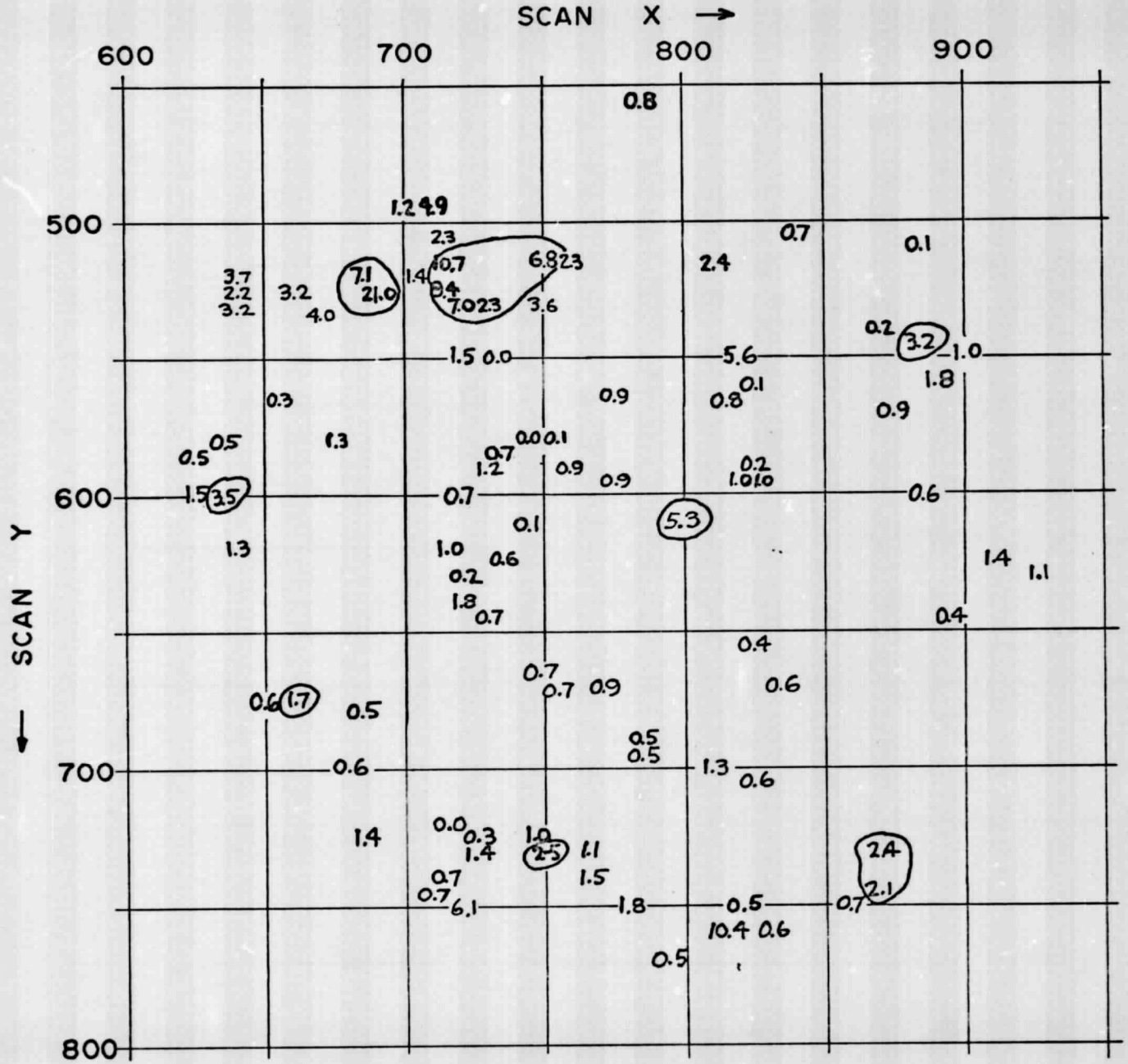
SCAN X →
600
700
800
900
500
600
700
800
SCAN Y
0.8
1.2 4.9
2.3
0.7
0.1
3.7
2.2
3.2
3.2
4.0
7.1
21.0
1.4
0.7
6.8 2.3
0.4
7.0 2.3
3.6
2.4
0.2
3.2
1.0
1.5
0.0
5.6
1.8
0.3
0.9
0.8
0.1
0.9
0.5
0.5
1.3
0.0
0.1
0.7
1.2
0.9
0.9
0.2
1.0 1.0
1.5
3.5
0.7
0.6
0.1
5.3
1.3
1.0
0.6
0.2
1.8
0.7
1.4
1.1
0.4
0.4
0.7
0.6
1.7
0.7
0.9
0.6
0.5
0.5
0.5
0.6
1.3
0.6
1.4
0.0
0.3
1.4
1.0
2.5
1.1
1.5
0.7
0.7
6.1
1.8
0.5
0.7
2.4
2.1
10.4
0.6
0.5

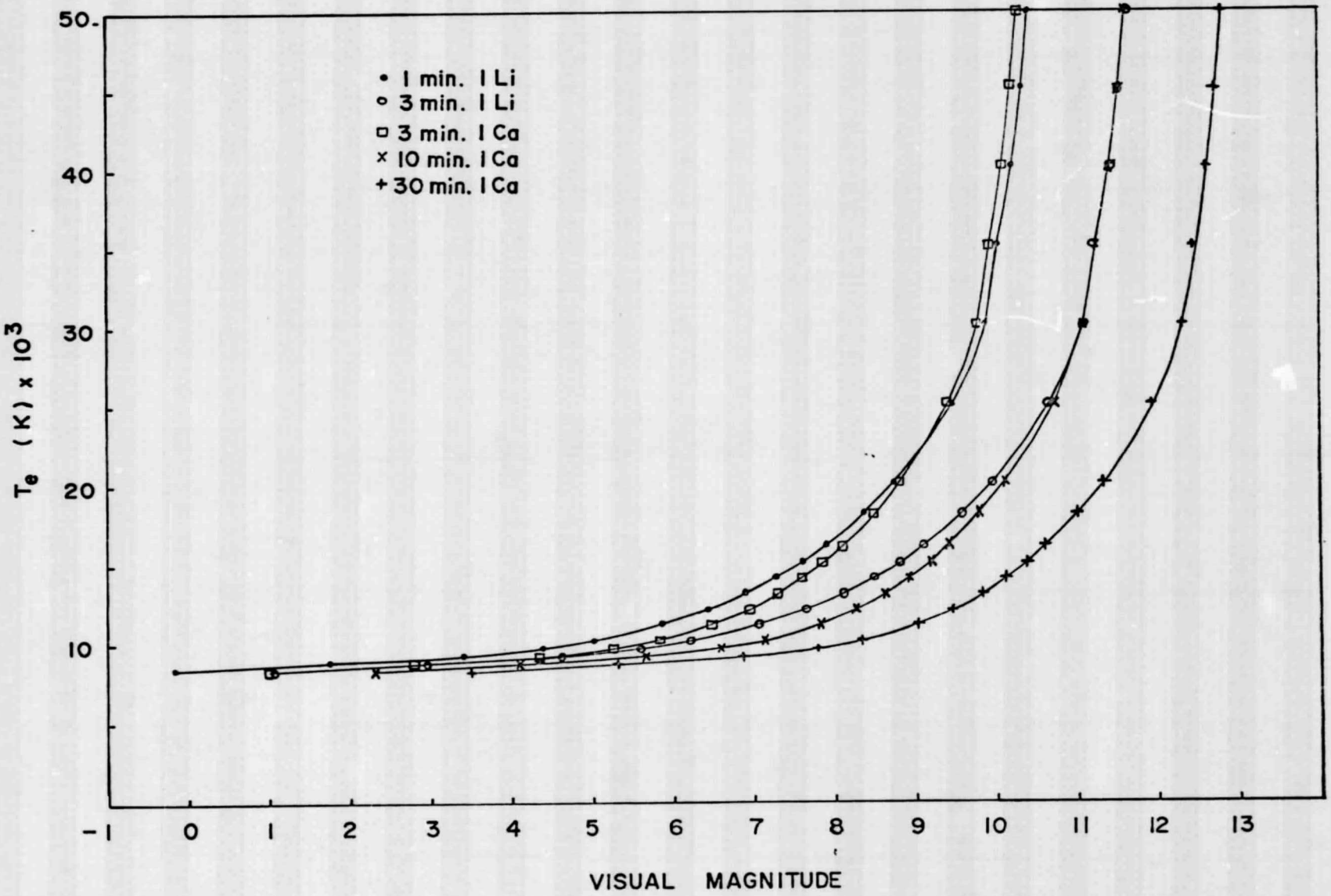
• 1 min. 1 Li
° 3 min. 1 Li
□ 3 min. 1 Ca
× 10 min. 1 Ca
+ 30 min. 1 Ca
T_e (K) x 10^3
50
40
30
20
10
-1
0
1
2
3
4
5
6
7
8
9
10
11
12
13
VISUAL MAGNITUDE

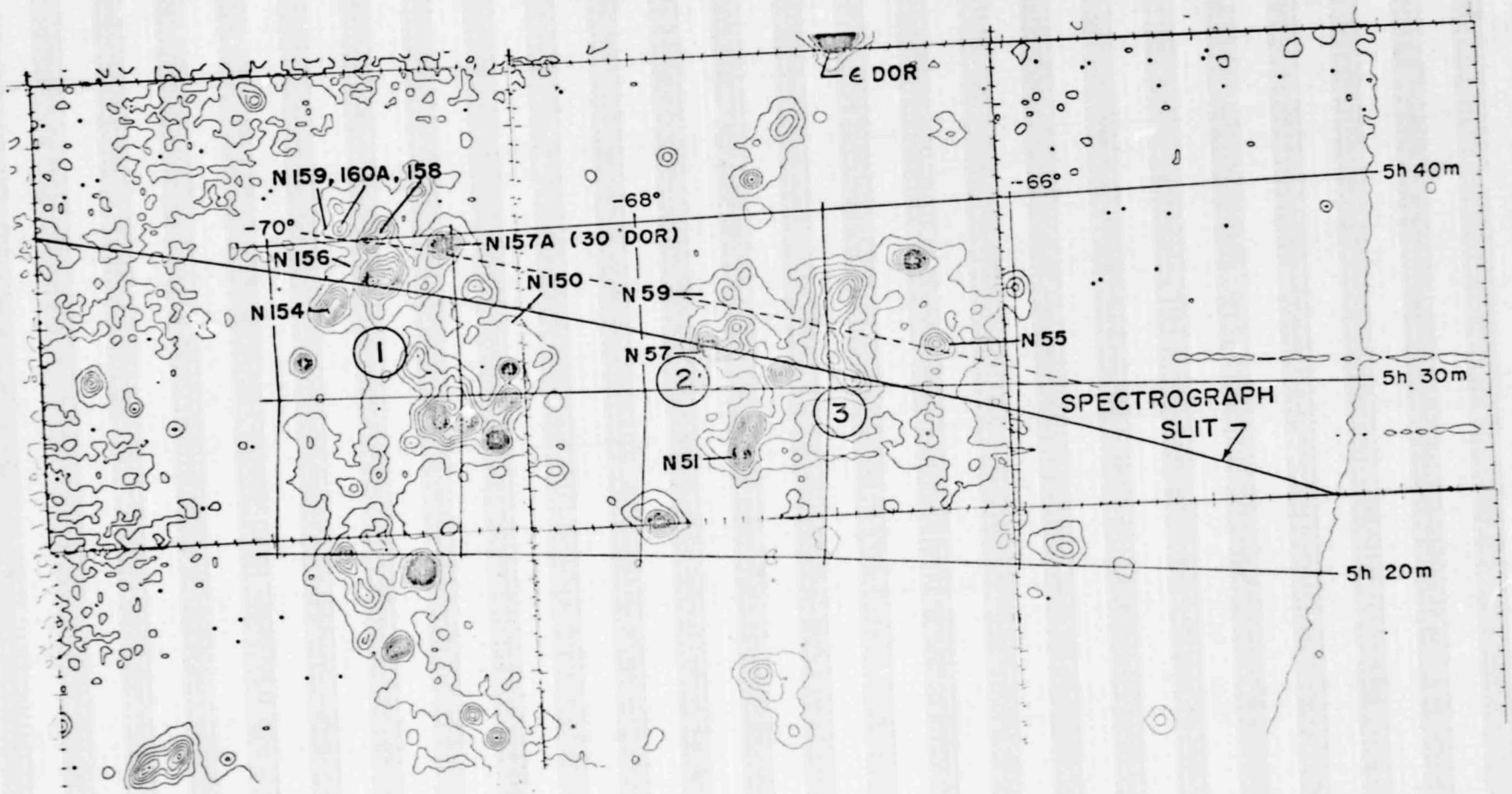
ε DOR
N159, 160A, 158
-70°
-68°
-66°
5h 40m
N157A (30 DOR)
N156
N150
N59
N154
N55
N57
5h 30m
1
2
3
SPECTROGRAPH
SLIT
N51
5h 20m